

1 Computational mechanisms underlying motivation to earn symbolic reinforcers
2

3 Abbreviated title: Motivation and symbolic reinforcers
4

5 Diana C. Burk¹, Craig Taswell¹, Hua Tang¹, Bruno B. Averbeck^{1†}

6 *1Laboratory of Neuropsychology, National Institute of Mental Health, National Institutes
7 of Health, Bethesda MD, 20892-4415*

8
9 Diana Burk, Ph.D.

10 E-mail: diana.burk@nih.gov

11 Contributions: Analyzed data, designed model, wrote manuscript
12

13 Craig Taswell, Ph.D.

14 E-mail: craig.taswell@nih.gov

15 Contributions: Collected data, edited manuscript
16

17 Hua Tang, Ph.D.

18 E-mail: hua.tang@nih.gov

19 Contributions: Collected data, edited manuscript
20

21 **†Correspondence to:**

22 Bruno B. Averbeck, Ph.D.

23 Laboratory of Neuropsychology, NIMH/NIH

24 Building 49 Room 1B80

25 49 Convent Drive MSC 4415

26 Bethesda, MD 20892-4415

27 E-mail: averbeckbb@mail.nih.gov

28 Contributions: Designed model, edited manuscript
29

30 Number of pages: 47

31 Number of figures: 9

32 Number of words (abstract): 213

33 Number of words (introduction): 527

34 Number of words (discussion): 1573
35

36 The authors declare no competing financial interests.
37

38 Acknowledgements: This work was supported by the Intramural Research Program of
39 the National Institute of Mental Health (ZIA MH002928 (BA)). The funders had no role in
40 study design, data collection and analysis, decision to publish, or preparation of the
41 manuscript.

42

43

44

45

46

47 **Abstract**

48 Reinforcement learning (RL) is a theoretical framework that describes how
49 agents learn to select options that maximize rewards and minimize punishments over
50 time. We often make choices, however, to obtain symbolic reinforcers (e.g. money,
51 points) that can later be exchanged for primary reinforcers (e.g. food, drink). Although
52 symbolic reinforcers are motivating, little is understood about the neural or
53 computational mechanisms underlying the motivation to earn them. In the present
54 study, we examined how monkeys learn to make choices that maximize fluid rewards
55 through reinforcement with tokens. The question addressed here is how the value of a
56 state, which is a function of multiple task features (e.g. current number of accumulated
57 tokens, choice options, task epoch, trials since last delivery of primary reinforcer, etc.),
58 drives value and affects motivation. We constructed a Markov decision process model
59 that computes the value of task states given task features to capture the motivational
60 state of the animal. Fixation times, choice reaction times, and abort frequency were all
61 significantly related to values of task states during the tokens task (n=5 monkeys).
62 Furthermore, the model makes predictions for how neural responses could change on a
63 moment-by-moment basis relative to changes in state value. Together, this task and
64 model allow us to capture learning and behavior related to symbolic reinforcement.

65

66 **Significance statement**

67 Symbolic reinforcers, like money and points, play a critical role in our lives. Like
68 rewards, symbolic reinforcers can be motivating and can even lead to compulsive
69 behaviors like gambling addiction. However, we lack an understanding of how symbolic

70 reinforcement can drive fluctuations in motivation. Here we investigated the effect of
71 symbolic reinforcers on behaviors related to motivation during a token reinforcement
72 learning task, using a novel reinforcement learning model and data from five monkeys.
73 Our findings suggest that the value of a task state can affect willingness to initiate a trial,
74 speed to choose, and persistence to complete a trial. Our model makes testable
75 predictions for within trial fluctuations of neural activity related to values of task states.

76

77 **Introduction**

78 In most decision-making contexts, the objective is to maximize rewards and
79 minimize punishments over time. In some situations, rewards are symbolic, such as
80 money or points, in which case they can be exchanged for primary rewards, such as
81 food or drink, in the future. Past studies have shown that animals and humans will work
82 for symbolic reinforcers, and symbolic reinforcers can drive learning and therefore
83 motivate behavior (Hackenberg, 2009, 2018).

84 Motivation is a process that invigorates behavior in the present to reach rewards
85 in the future (Berridge, 2004; Berke, 2018; O'Reilly, 2020). Motivation can be studied in
86 the context of reinforcement learning (RL). Learning builds predictions of choice
87 outcomes that can be used to direct future behavior (Sutton and Barto, 1998). N-armed
88 bandit tasks are often used to study RL in animals. These tasks can be modeled with
89 Rescorla-Wagner (RW) RL models (Rescorla, 1972), because the choices lead
90 probabilistically, but immediately, to a primary reinforcer (Bartolo and Averbeck, 2020;
91 Beron et al., 2022). However, one can also use symbolic reinforcers, for example,
92 tokens or money to drive learning (Jackson, 1996; Kirsch et al., 2003; Seo and Lee,

93 2009; Delgado, Jou and Phelps, 2011; Taswell et al., 2018; Taswell et al., 2021;
94 Falligant and Kranak, 2022; Yang, Li and Stuphorn, 2022; Taswell et al., 2023). In these
95 tasks, subjects learn to make choices to obtain tokens, which can be exchanged in the
96 future for primary reinforcers. Token based learning tasks set up a distinction between
97 two types of cues that predict rewards in different ways. Specifically, tokens predict
98 rewards on long-time scales, deterministically, whereas choice cues predict tokens.
99 Furthermore, the relation between cues and tokens must be learned. Such tasks
100 involving symbolic reinforcement cannot be accurately captured with current RL models,
101 because the distinction between rewards and symbolic reinforcers cannot be made
102 explicit.

103 Thus, we developed a Markov Decision Process (MDP) model to characterize
104 the value of symbolic reinforcers, and the computational mechanism that links cues
105 through tokens to rewards. The MDP also allows us to model multiple factors that drive
106 value, including the time to reach primary rewards, and the probability of obtaining
107 additional rewards in the future. We can therefore use the model to establish which
108 factors most strongly drive behavior. To establish the validity of the model, beyond
109 predicting learning which can be done with RW-RL models, we examined the
110 relationship between the state value (i.e. the expected discounted sum of future
111 rewards) and behavioral measures associated with motivation. Five monkeys performed
112 a task where they learned to select images that led to gaining or losing tokens. The
113 tokens were later exchanged for juice rewards. To examine the ability of the model to
114 capture motivation, we conducted regressions between state value and change in state
115 value and three behaviors linked to motivation. To demonstrate the effect of each task

116 dimension included in the model, we performed marginalization analyses, where each
117 feature was removed and the analyses were repeated. These analyses demonstrated
118 that all features that drove value in the model contributed to motivation. Taken together,
119 our results make predictions for how neural activity might evolve in reinforcement
120 learning circuits during a task involving symbolic reinforcement.

121

122 **Materials and Methods**

123

124 **Subjects**

125 The subjects included three male and two female rhesus macaques with weights
126 ranging from 6 to 11 kg. Four monkeys were used as control monkeys in a previous
127 study (Taswell et al., 2018). One additional monkey was a naïve monkey whose first
128 task was the tokens task. For the duration of collecting behavioral data, monkeys were
129 placed on water control. On testing days, monkeys earned their fluid from performance
130 on the task. Experimental procedures for all aspects of the study were performed in
131 accordance with the Guide for the Care and Use of Laboratory Animals and were
132 approved by the National Institute of Mental Health Animal Care and Use Committee.

133

134 **Experimental Design**

135 We conducted post hoc analyses on previously published data (Taswell et al.,
136 2018) and data from one additional subject. We use data from one variant of the tokens
137 task, previously called Stochastic Tokens with Loss (referred to as TkS).

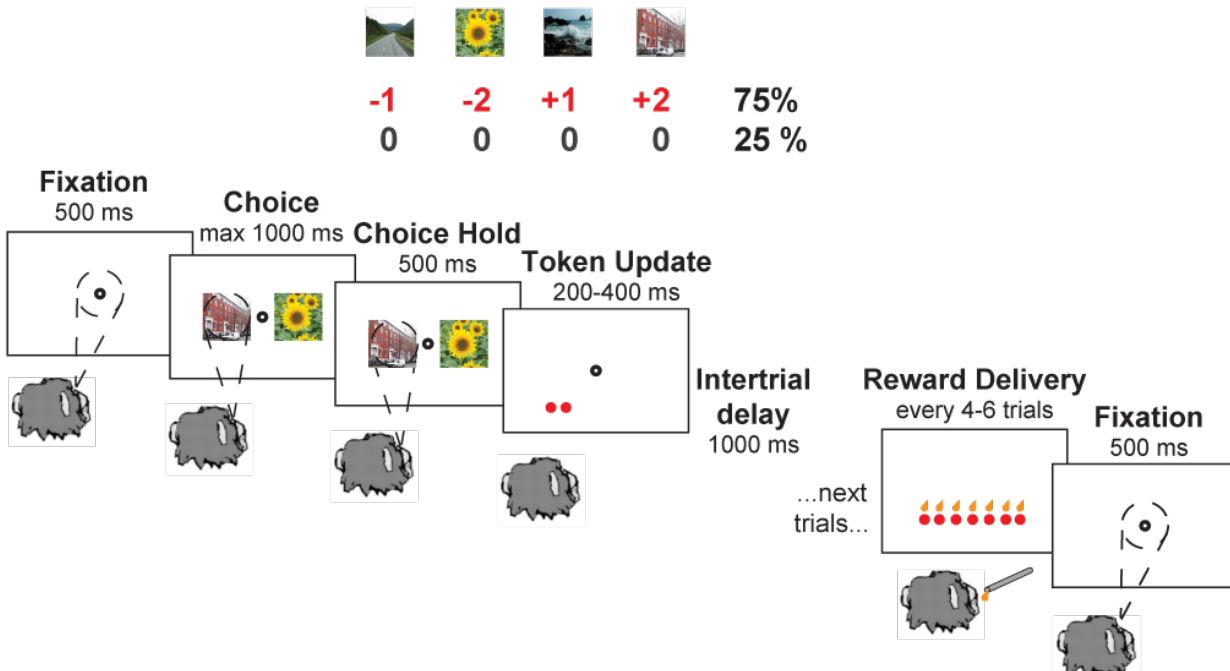
138 The images used in the task were normalized for luminance and spatial
139 frequency using the SHINE toolbox for MATLAB (Willenbockel et al., 2010). Image
140 presentation was controlled by PC computers running Monkeylogic toolbox (Version
141 1.1) for MATLAB (Asaad and Eskandar, 2008; Hwang, Mitz and Murray, 2019). Eye
142 movements were monitored using the Arrington ViewPoint eye-tracking system
143 (Arrington Research).

144

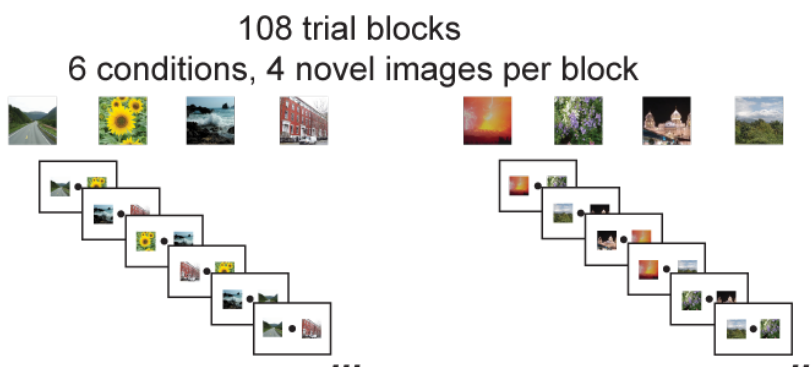
145 **Stochastic Tokens Task with Gains and Losses**

146 Blocks consisted of 108 trials that used four novel images that had not been
147 previously presented to the animal. Each image was associated with a token outcome
148 (+2, +1, -1, -2), such that if that image was chosen, the animal gained or lost the
149 corresponding number of tokens 75% of the time and received no change in tokens
150 25% of the time (**Fig. 1A**).

A



B



151

152 **Figure 1. Overview of the Tokens task with stochastic rewards. (A)** Flow of single trial. First
 153 the monkey fixates on the screen and is required to hold fixation for 500 ms. Two cue images
 154 appear on either side of fixation, each of which is associated with gaining or losing tokens (+2,
 155 +1, -2, -1). The monkey must make a saccade to one of the images and hold their gaze for 500
 156 ms. After a successful hold, the number of tokens associated with the chosen option appears on
 157 the screen 75% of the time, and 25% of the time, nothing changes. After a 1000 ms intertrial
 158 delay, the next trial begins. Every four to six trials, tokens were exchanged for juice drops 1:1
 159 and the monkey started the subsequent trial with zero tokens. **(B)** The monkeys learned through
 160 trial and error which visual images were associated with gaining tokens and which images were
 161 associated with losing tokens. Four new images were presented every block of 108 completed
 162 trials. Each pair of cues (six total) was seen 18 times (nine Left/Right, nine Right/Left). Image
 163 credit: Wikimedia Commons (scene images).

164

165 On each trial, monkeys had 2000 ms to acquire a fixation spot at the center of the
166 screen and were required to hold fixation for 500 ms. After monkeys held central
167 fixation, two of the four possible images would appear to the left and the right of
168 the fixation point. The animal had 1000 ms to choose one of the images by making a
169 saccade to an image and hold their gaze on the image for 500 ms to indicate their
170 choice. If the monkey moved his eyes outside the fixation window during fixation, did not
171 choose a cue, or did not hold the cue long enough, the trial was aborted and repeated
172 immediately. After a successful hold of gaze on a choice, tokens associated with the
173 image were then added or subtracted from their total count, represented by circles at
174 the bottom of the screen. Note that the animals could not have fewer than zero tokens.
175 After an intertrial interval of 1000 ms, the next trial would begin with the accumulated
176 tokens visible on the screen the entire time. Every four to six trials, tokens were
177 exchanged 1:1 for juice drops. During this cashout epoch, one drop of juice was
178 delivered and a token disappeared, until all tokens were gone. The animal did not
179 choose when to cash out, rather the probability of exchanging tokens for juice drops
180 was a uniform distribution over four to six trials.

181 There were six cue conditions in the task, defined by the possible pairs of the
182 four images. The conditions within a block were presented pseudorandomly, such that
183 the animals saw each condition twice (same images, opposite sides) every 12 trials
184 before seeing any condition a third time. This prevented strings of trials with loss v. loss
185 that could lead to aberrant behaviors. At the end of each 108-trial block, we introduced
186 four new images and the animals restarted learning associations between the pictures
187 and the token outcomes (**Fig. 1B**). The animals completed approximately 9 blocks of

188 images per session, and approximately 20 sessions from each animal were used for
189 subsequent analyses.

190

191 **Model Framework**

192 We modeled the Tokens task using a Markov decision process with partially
193 observable states (POMDP). To fit the POMDP to each animal's behavior, we leveraged
194 the Rescorla Wagner Reinforcement Learning Model (RW-RL) to calculate the average
195 values of each of the four cue images and to verify the validity of our MDP results for
196 fitting choice probability curves across the cue conditions. Details of this process are in
197 the following sections.

198

199 **Rescorla Wagner Reinforcement Learning (RW-RL) Model**

200 We used a variant of the RW-RL model as was previously used to model the
201 tokens task (Taswell et al., 2018).

202 We fit a Rescorla-Wagner value update equation given by the following:

$$203 \quad v_i(t+1) = v_i(t) + \alpha_i(R - v_i(t)) \quad (1)$$

204 where the variable v_i is the value estimate for cue option i , R is the change in the
205 number of tokens that followed the choice in trial t , and α_i is the cue-dependent learning
206 rate parameter. In past work on this data, the model with a separate learning rate
207 parameter for each cue was found to be the best RW-RL model fit to the data. Thus, we
208 continued using this formulation of the RW-RL for these analyses, although the results
209 described in this study are not contingent on this choice.

210 The value computed in Eq. 1 were then used to compute choice probabilities for
 211 each cue pair using the softmax function:

212
$$d_j(t) = (1 + e^{\beta^{RW}(v_i(t) - v_j(t))})^{-1}, d_i(t) = 1 - d_j(t)$$

 213 (2)

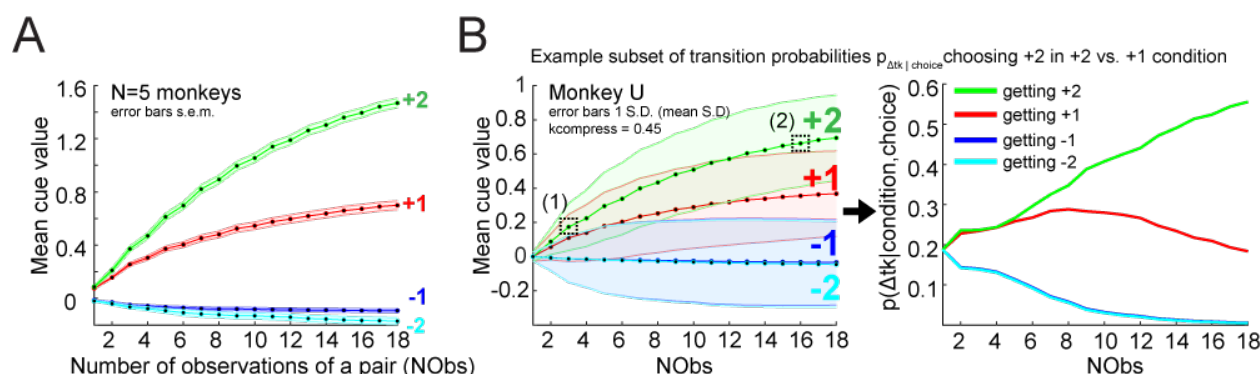
214 where β , is the consistency choice parameter, fit across all six cue conditions, and i and
 215 j are the two choice options. We then maximized the likelihood of the animal's
 216 choices, D , given the parameters, using the cost function:

217
$$f(D|\alpha_i, \beta^{RW}) = \prod_t [d_1(t)c_1(t) + d_2(t)c_2(t)]$$

 218 (3)

219 where $d_1(t)$ is the choice probability value for option 1 on trial t and $c_1(t)$ and $c_2(t)$ are
 220 indicator variables that take on a value of 1 if the corresponding option was chosen and
 221 0 otherwise. This model was fit across blocks in each session for each monkey to give
 222 one set of fit parameters for each session.

223 Mean cue values as a function of learning trial in each block from the RW-RL
 224 model were used to generate transition probabilities for the MDP discussed in detail
 225 below. To extract mean cue values, all v_i for a single cue were averaged across
 226 sessions. This produced four curves that reflected the change in cue value across trials
 227 for each animal (**Fig 2A, 2B**).



228

229 **Figure 2. Mean cue values extracted from the RW-RL model and transition probabilities**
230 **for change in tokens given a cue image selection. (A)** Mean cue values across number of
231 observations of a cue pair (NObs) are plotted for each of the four cues in the stochastic tokens
232 task (error bars s.e.m. across monkeys). The +2 curve is the highest, followed by the +1 curve,
233 reflecting how the animals learned to select the +2 and +1 image cues. -2 and -1 curves are
234 similar, reflecting that the animals did not learn the value differences between the -2 and -1 cue
235 options. The mean values were extracted from the RW-RL model fits to each monkey. Each
236 data point is an average of the three conditions in which the cue was observed. For example, for
237 the +2 curve, a single data point would be the average value of the +2 cue value from the
238 conditions +2 v +1, +2 v -2, +2 v -1. **(B)** Example set of curves from Monkey U with scaling
239 applied to the variance (see Methods) and scaling parameter fit during the MDP fitting process
240 and derivation of a subset of transition probabilities. Left: (1) +2 cue value highlighted early in
241 learning at trial 3. (2) +2 cue highlighted late in learning at trial 16. Error bars are the mean
242 variance across blocks and solid lines show the cue values with the parameterized scaling
243 factor. Right: Plot of a subset of transition probabilities derived from mean value curves for the
244 +2 v +1 condition and choice of +2 for each possible token outcome. $p(\Delta tk=0|choice +2 cue)$ is
245 always 0.25 and is not shown.

246

247 **Markov Decision Process (MDP) Model**

248 The MDP model computes the value of each task state. Task states were
249 defined by four features of the task: number of tokens (NTk), trials since cashout
250 (TSCO), task epoch (TE), and number of observations of a cue pair (NObs). The state
251 space included all possible combinations of these features across a single block of
252 trials, such that the bounds for each feature were: NTk: 0-12, TSCO: 1-6, TE: 1-10
253 (which included fixation, 6 cue conditions, token outcome, cashout, intertrial interval),
254 NObs: 1-18. Using NObs as a feature allowed us to avoid having to track each time a
255 cue was shown, chosen and rewarded across trials, and to reduce the size of the state
256 space by 18^{12} states, which also made a tabular form of the model tractable. The model
257 of the task was in epoch time (i.e. event based), rather than true time (i.e. seconds
258 based).

259 The state space can be considered as a graph with edges and nodes, where the
260 states are defined by the possible combinations of these features, and the edges are
261 the transitions to future states. A trajectory through the state space represents one trial

262 and as the model proceeds through a block, the trajectory traverses through the state
263 space.

264 The state value, sometimes called state utility, $u(s_t)$, was calculated using the
265 equation:

266
$$u(s_t) = \max_{a_t \in A} [r(s_t, a_t) + \gamma \sum_{j \in S_{t+1}} p(j|s_t, a_t)u(j)] \quad (4)$$

267 where s_t is the state, a_t is the action taken at that state, $u(s_t)$ is the state value, $r(s_t, a_t)$
268 is the immediate reward, γ is the discount factor, $p(j|s_t, a_t)$ is the transition probability to
269 future state j and S_{t+1} is the set of immediate future possible states from state s_t . A
270 range of discount factors ($\gamma=0.8, 0.85, 0.9, 0.95, 0.99, 0.999$) were tested. $\gamma=0.999$
271 produced the least error for the regressions and was used for all analyses. We used
272 value iteration to fit the MDP (Puterman, 2014). The algorithm loops over all possible
273 states and recomputes Eq. 4 until both the policy and state values converged. This took
274 approximately 100 iterations across the state space for each MDP that was fit.

275 The transitions between states include: fixation to the six cue states, cue state to
276 token update, token update to cashout or intertrial interval and intertrial interval to
277 fixation. The transition probabilities from fixation to any cue state were modeled as
278 $p_{cues}=1/6$ as there were 6 possible cue pairs. The transition probabilities from token
279 update to cashout were $p_{cashout}=0$ for TSCO 1-3, $p_{cashout}=0.33$ for TSCO 4, $p_{cashout}=0.50$
280 for TSCO 5, $p_{cashout}=1.0$ for TSCO 6. Transition probabilities for the transition to a
281 change in tokens given a cue image selection, i.e. $p(\text{change in tokens} | \text{image choice in}$
282 a given condition), were fit using the behavioral data and average cue values that were
283 extracted from the RW-RL model fits. Thus, this is not an ideal observer estimate, but
284 rather our inference of the monkey's estimate. These transition probabilities represent

285 the monkey's mapping of individual cues to outcomes, i.e. which picture leads to +2
286 tokens. The cue values are related to this mapping, thus making the RW-RL values an
287 approximation to the process by which the animal learns the outcomes related to each
288 cue image (**Fig. 2**).

289 We had to infer the monkey's estimate of the number of tokens they would
290 receive when they chose a given option. For example, in the first trial of a new block,
291 the monkeys had no experience with any options, and therefore they should assume
292 that choice of any option could lead to either -2, -1, 0, 1, or 2 tokens. However, after 10
293 trials the monkeys had a reasonable estimate of the token outcomes associated with
294 each option. This process makes the MDP have partially observable states, as we
295 estimate the transition probabilities using mean values from the RW-RL model. We
296 carried out this estimate in two steps. First, we calculated the value estimates for each
297 option, as a function of the number of trials they had seen each option using the RW-RL
298 algorithm value estimates (Fig. 2). We then used these estimates to calculate the
299 posterior probability that choice of a given cue would lead to a given outcome (i.e. Δtk).
300 For the outcome of no tokens, $p(\Delta tk = 0) = 0.25$. For all other possible outcomes, the
301 following equations were used:

302
$$p(\Delta tk = \{+2, +1, -2, -1\}) = \frac{0.75}{4} \quad (5)$$

303

304
$$p(\Delta tk | v_{cue}) = \frac{p(v_{cue} | \Delta tk) p(\Delta tk)}{p(v_{cue})} \quad (6)$$

305
$$p(v_{cue} | \Delta tk = j) = \frac{1}{\sigma \sqrt{2\pi}} e^{(-\frac{1}{2} \frac{(x_{cue} - \mu_j)^2}{\sigma^2})} \quad (7)$$

306

307
$$p(v_{cue}) = \sum_{j=1}^4 p(v_{cue} | \Delta tk_j) p(\Delta tk_j) \quad (8)$$

308 and where v_{cue} is the mean value of a single cue for a given NObs, $\Delta tk = +2, +1, -1, -2$,
309 x is the mean of the cue value of the chosen option, and μ is a mean value of one of the
310 other cues. Transition probabilities were calculated for all possible choices and NObs
311 and were not dependent on other MDP features such as NTK or TSCO. For example, 3
312 trials into the block, mean cue values were 0.17, 0.11, -0.01, -0.01 for the +2 cue, +1
313 cue, -1 cue, and -2 cue, respectively (Fig. 2B). To calculate $p(\Delta tk = +2 | v_{cue} = 2)$ (i.e.
314 the probability of receiving 2 tokens for choosing the +2 cue), $x=0.17$, $\mu_1=0.11$, $\mu_2= -$
315 0.01 , $\mu_3=-0.01$, which produces $p(\Delta tk = +2 | v_{cue} = 2)=0.24$ in the +2 versus +1
316 condition. Later in the block, for example on NObs=16, mean cue values were 0.66,
317 0.36, -0.03, -0.04 for the +2 cue, +1 cue, -1 cue, and -2 cue, respectively. At this point in
318 learning, $p(\Delta tk = +2 | v_{cue} = 2)= 0.52$ in the +2 versus +1 condition.

319 The mean cue values were used to fit the set of transition probabilities
320 $p(\Delta tk | \text{choice})$ for $\Delta tk = 0, 1, 2, -1, -2$ and $\text{choice} = \text{cue 1, cue 2}$. First, an MDP was fit
321 using the mean cue values for each animal in order to compute a converged policy of
322 choices and action values without any free parameters. These MDP models captured
323 general trends of behavior to select the better options (i.e. an optimal MDP) but showed
324 faster learning than the animals learned. To better match animal learning behavior, we
325 optimized the transition probabilities underlying the behavioral performance of the MDP.

326 To optimize the set of transition probabilities $p(\Delta tk | \text{choice})$, mean cue values
327 were used with two free parameters: (1) a scaling parameter for the mean cue values
328 such that:

329
$$v_{cue}^s = k * v_{cue} \quad (9)$$

330 for all mean cue values and (2) an inverse temperature parameter for the choice
331 probability (β^{MDP}). In addition, the variance on the mean value curves for each animal
332 was set to the average variance across all four cues, allowing variance to vary across
333 trials, but not across cue values. Using the initial MDP fit and the behavioral data from
334 the task for each animal, the two free parameters were fit jointly by minimizing the error
335 between the MDP choice probability and average performance across sessions for each
336 monkey (**Table 1**). The resulting parameters and transition probabilities were then used
337 to refit the MDP until the state values and policy reconverged.

Monkey	Mean value scaling parameter (k)	Choice probability parameter (β^{MDP})
Monkey U	0.45	2.77
Monkey B	0.71	1.87
Monkey S	1.04	1.15
Monkey P	1.14	1.34
Monkey A	0.53	2.24

338 **Table 1. MDP free parameter values for each monkey.** Two parameters were optimized to
339 minimize the error between the MDP choice probability and the monkey's choice behavior. The
340 mean value scaling parameter acted as a scalar on the variance of the value curves (Eq. 9).
341 The choice probability parameter was the inverse temperature parameter used to calculate the
342 choice probability using action values derived from the MDP.
343

344 In addition, MDP models were fit using a range of discount factors ($\gamma = 0.8, 0.85,$
345 $0.9, 0.925, 0.95, 0.99, 0.999$) for each animal's dataset. To determine the discount
346 factor that produced the best fit to behavior, each γ was used to regress on fixation
347 reaction times, choice reaction times, $p(\text{Abort})$ and to produce choice probability curves
348 for the six conditions (see below for details on the regressions). For all monkeys, $\gamma =$
349 0.999 produced the best fits to these behavioral data metrics, and thus, $\gamma = 0.999$ was
350 used for all models.

351

352 **Regressions and Statistical Analyses**

353 Comparison of performance of the MDP and RW models at predicting choice
354 behavior was conducted using a comparison of correlation coefficients. Correlation
355 coefficients (r_1, r_2) were calculated between the average choice behavior and each
356 model separately. The values were then Fisher-z transformed to compute a p value for
357 a two-sided test for differences between the correlation coefficients.

358 State values were extracted for all trials and epochs using the MDP fits for each
359 animal. This produced a table of states such that the value of each state was: $u(s_t) =$
360 $f(NTk, TSCO, TE, NObs)$. These state utilities were used to characterize trial-by-trial
361 relationships to reaction time to acquire fixation, choice reaction time, and trial aborts.

362 Mean reaction times (RT) were computed by averaging reaction times across
363 blocks of trials and then averaging across sessions for each monkey. Scatter plots of
364 RTs from individual sessions do not include outlier reaction times. Outlier RTs were
365 removed using Tukey's method: $RT > q0.75 + 1.5 * IQR$ and $RT < q0.25 - 1.5 * IQR$, where
366 IQR is the interquartile range.

367 To assess the relationship between state value and reaction times to acquire
368 fixation, linear regression on state value was performed such that:

$$369 \log(RT_{acquire_fixation}) = \beta_0 + \beta_{V_{Fix}} V_{fix} \quad (9)$$

370 where V_{fix} is the value of the fixation state. Reaction times were log transformed before
371 the regression.

372 To assess the relationship between state value and reaction times to choose,
373 linear regression on state value was performed such that:

$$374 \log(RT_{acquire_fixation}) = \beta_0 + \beta_{V_{cue}} V_{cue} + \beta_{\Delta V} (\Delta V) \quad (10)$$

375 where V_{cue} is the value of the cue presentation state and $\Delta V = V_{cue} - V_{fix}$. Reaction
376 times were log transformed before the regression.

377 To assess the relationship between state value and the probability of aborting a
378 trial, logistic regression on state value was performed such that:

379
$$p(\text{Abort}) = (1 + e^{-(\beta_0 + \beta_{V_{cue}} V_{cue} + \beta_{\Delta V} (\Delta V))})^{-1} \quad (11)$$

380 where V_{cue} is the value of the cue presentation state and $\Delta V = V_{cue} - V_{fix}$. We
381 additionally assessed the effect of cue condition on $p(\text{Abort})$ using a mixed effects
382 ANOVA, where monkey was the random effect and cue condition was the fixed effect.

383 To assess whether regressors were significantly different than zero, for each
384 animal, t-tests on the distributions of beta values across sessions for each regressor
385 were performed for each animal. These values are reported in the text. Mean
386 parameter values did not appear to be Gaussian distributed across monkeys.

387 Therefore, to assess whether the regressors were significantly less than zero at the
388 group level, the non-parametric Wilcoxon signed-rank test was used on the distribution
389 of mean parameter values across animals. Results of these tests are reported in the
390 figure captions and text. To show group trends in relationships between reaction times
391 and regressors, 1D kernel smoothing was conducted on each monkey's data with $\sigma =$
392 0.5 with a Gaussian kernel.

393 We also sought to examine the contributions of the different variables that
394 defined the state to each regression by marginalizing over one factor at a time, to
395 remove its effect, and carrying out the correlation analyses. To perform this
396 marginalization, we averaged over the state values for all possible values of a single
397 feature, given the other features. For example, to compute state values for all features

398 averaging over NTk, with $TSCO = 4, TE = 1, NObs = 12$, we computed $V_{fix} =$
399 $\text{mean}(f(NTk = 0:8, TSCO = 4, TE = 1, NObs = 12))$, as NTk=8 is the maximum number
400 of tokens possible when TSCO=4.

401

402 **Code Accessibility**

403 All code used to generate the results in this manuscript can be accessed on GitHub
404 here: https://github.com/dcb4p/mdp_tokens.

405

406 **Results**

407 Five monkeys were trained on a stochastic tokens task (Taswell et al., 2018)
408 (**Fig. 1**). Briefly, each block of the task used four novel images, and choice of each
409 image led to a different possible token outcome (+2, +1, -1, -2). In each trial, two of the
410 four images were presented as options, and the monkey made a saccade to one of the
411 cues and held their gaze to indicate their choice. After the choice, the monkey received,
412 stochastically, the corresponding change in tokens on the screen. In 75% of the trials
413 they received the number of tokens associated with the cue and in 25% of the trials the
414 number of tokens did not change. Every four to six trials was a cashout trial. In cashout
415 trials, the monkey received one drop of juice for each accumulated token. The monkey
416 would then start over accumulating tokens until the next cashout trial. Each of the pairs
417 of cue images (six total) were presented 18 times during a block of trials. At the end of
418 the block, the four cue images were replaced with novel images, and the monkey
419 restarted learning the associations between the images and token outcomes.
420 Behavioral performance and learning were assessed for each animal by the increasing

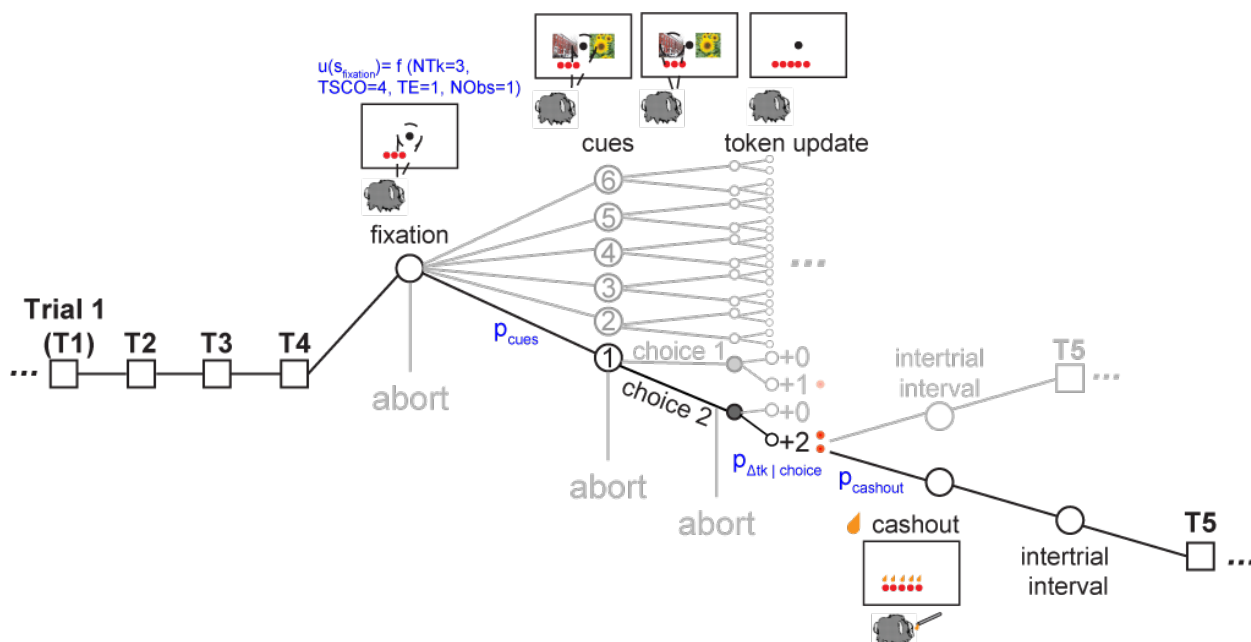
421 frequency with which the monkeys chose the image associated with the better option in
422 each condition over the course of a block.

423 In this task the monkeys were not given rewards on every trial. Rewards were
424 only given at the time of cashout when tokens were exchanged for juice. Commonly
425 used RL models, such as the Rescorla Wagner model (RW) (Sutton and Barto, 1998),
426 do not make a distinction between symbolic reinforcers and primary rewards and
427 therefore they do not have a natural way to model the difference between primary and
428 secondary reinforcers. To address this, we developed a state-based, Markov decision-
429 process model of the stochastic tokens RL task to capture the relevant features of the
430 task that would affect motivation and choice behavior. Within MDP models, values and
431 available actions are defined by the current state. In our model, the state is a function
432 of the number of tokens (NTk), trials since cashout (TSCO), task epoch (TE) and
433 number of observations of each condition within the block (NObs). The state space
434 consists of all possible combinations of these four features. The model, once trained,
435 has states that inherit value from their proximity to the true rewarding state (cashout),
436 similar to how a well-trained monkey expects to earn juice in the future.

437 State values are given by the maximum action value in each state. State values
438 and action values are equivalent in all epochs except the choice epoch, because only
439 one action is possible in the other epochs. Rewards are only delivered in the cashout
440 period, and therefore immediate expected values, $r(s_t, a_t)$ are 0, except in the cashout
441 period when more than 0 tokens have been accumulated. In all other states, immediate
442 expected values are 0, and state values are future discounted expected values, all of
443 which are filtered through the graph from the cashout period. Thus, future expected

444 values in each state follow from the features of the task that predict the delay to and
 445 size of the reward that will be delivered in cashout.

446 For example, the value of the fixation state is a combination of the number of
 447 tokens accumulated, trials since cashout, and number of observations of the cue pairs
 448 witnessed up until that trial (Fig 3). The value of the fixation state is the sum of the
 449 immediate expected value (which is 0 at fixation because no juice is ever delivered) and
 450 the future expected value, which is the expected value of the next state (i.e. the average
 451 over the cue states, each of which occurs with a probability of 1/6). Thus, state value in
 452 the fixation state is inherited from the values of the cue states.



453

454 **Figure 3. Overview of task state space for Markov Decision Process (MDP) framework.**
 455 Each circular node represents a state given by a set of task features: token count (NTk), trials
 456 since cashout (TSCO), task epoch (TE), number of cue condition observations (NObs). Each
 457 edge of the graph represents a transition probability, or the transition between states that could
 458 be deterministic ($p=1$) or probabilistic ($p < 1$). A single trial is highlighted and the progression
 459 from each step in the task is shown for an example trial that ends in a cashout. The example
 460 trial starts at fixation and the monkey has three tokens, making the value of the state $f(NTk=3,$
 461 $TSCO=4, TE=1, NObs=1)$. The transition probability $p_{cues}=1/6$ and represents the probability of
 462 any of the six cue conditions being the next state. At the cue states, the monkey must make a
 463 choice, and the model captures this choice policy behavior. The next set of states after the cue
 464 state is the outcome state; the transition is governed by the transition probability $p_{\Delta tk|choice}$. In

465 the example, the monkey receives 2 tokens and the model receives 2 tokens. After the outcome
466 state, the monkey can transition to the intertrial interval or cashout; the transition to this state is
467 governed by p_{cashout} . During cashout, one drop of juice is exchanged for each token and all the
468 tokens disappear before proceeding to the next intertrial interval and subsequent trial. Image
469 credit: Wikimedia Commons (scene images).

470

471 In each cue state, there is a choice between the two cues, which then leads to
472 the token outcome states. As five of the six possible cue conditions have gain
473 outcomes (once the monkey learns to select the better option), the state values of the
474 cue conditions reflect this possible gain as it develops with learning. In the outcome
475 states the monkey can receive +2, +1, 0, -1, or -2 tokens. As there is also no immediate
476 reward available during the cue states, state value comes from the future expected
477 value of the intertrial interval or cashout states.

478 The monkey learns to choose options that maximize gaining tokens over losing
479 tokens. We modeled this learning as an inference over the token outcome distribution
480 associated with each choice, using a parameterized function of the number of times an
481 option had been chosen. The model, which generated an estimate of the transition
482 probabilities from cue to token outcome ($p_{\Delta\text{tk}|\text{choice}}$), was fit to each monkey's choice
483 behavior. Unlike the transition from the fixation state to the cue state (p_{cue}), the
484 probability of transitioning to each outcome state ($p_{\Delta\text{tk}|\text{choice}}$) changes as the monkey
485 learns the associations between the cue options and token outcomes. For example, at
486 the start of a block, the monkey does not know which cue image predicts which token
487 outcome, and $p_{\Delta\text{tk}=+2|\text{choice}} = p_{\Delta\text{tk}=+1|\text{choice}} = p_{\Delta\text{tk}=-2|\text{choice}} = p_{\Delta\text{tk}=-1|\text{choice}}$. Once the monkey
488 learns which cue image is associated with +2 tokens, they are more likely to select that
489 option, and we assume they infer that the probability of getting two tokens, $p_{\Delta\text{tk}=+2|\text{choice}}$,
490 is larger given choice of that option. Thus, the transition probabilities change over the

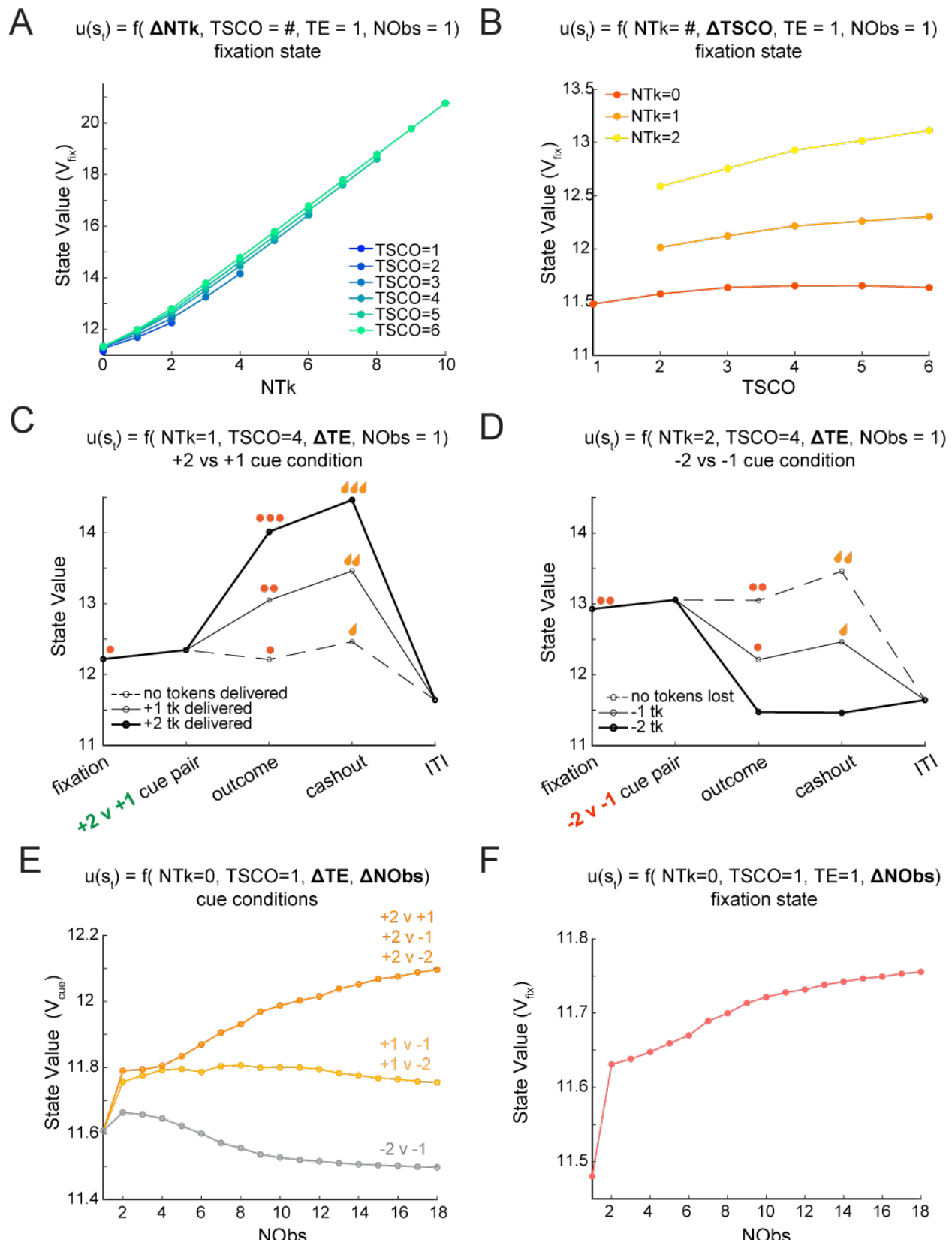
491 course of a block as the number of times the cue pair has been observed (NObs)
492 increases. The changes in these transition probabilities reflect learning (Fig. 2B,C).

493 At the time of token outcome, the next possible states are either the intertrial
494 interval or cashout, governed by the transition probability p_{cashout} . This transition is a
495 feature of the task and does not change with learning. At the time of cashout, the state
496 value is the sum of the immediate reward (1 drop of juice per token present) and the
497 next state, which is the intertrial interval, with zero tokens. In the model, this means
498 state value will drop after cashout if the monkey cashed out tokens for juice, as the state
499 value depends on the number of tokens.

500

501 **Changes in task features drive fluctuations in state value**

502 State values change with variation of each state feature. For example, having
503 more tokens increases state value (**Fig. 4A**). Being closer to the cashout state (e.g.
504 TSCO >4) also increases state value (**Fig 4B**). As the monkey proceeds through the
505 task epochs (i.e. fixation, cue onset, outcome, cashout or intertrial interval), the state
506 value will also increase for conditions where tokens can be gained, and more subtly,
507 because one is also getting closer to cashout (**Fig. 4C**). For the -2 v. -1 cue condition
508 where tokens can only be lost or maintained (if there is a no change outcome), the
509 value of the state either decreases or increases marginally approaching cashout (**Fig**
510 **4D**). In the first trial of a block, when the monkey has started learning the associations
511 between cues and outcomes (i.e. NObs =1), the best option in a pair of cues will be
512 ambiguous. This is reflected by identical state-action values in the model (**Fig. 4E**).
513 Near the end of the block, when the monkey



515 **Figure 4. How changes in state features can affect state value (example from Monkey B).**
516 **(A)** Fixation state value (V_{fix}) versus token count (NTk). As NTk increases, state value
517 increases. For one trial since cashout (TSCO=1), only 1 trial has been completed, so the
518 maximum number of tokens available is two. As the TSCO increases, juice will be delivered
519 sooner, which is reflected by higher state value. **(B)** Fixation state value (V_{fix}) versus trials since
520 cashout (TSCO). As TSCO increases, the state value increases when there is more than one
521 token (NTk=1, NTk=2). If there are zero tokens (NTk=0), then state value increases until
522 TSCO=4. When cashout becomes possible, state value begins to decrease when there are no
523 tokens, because a cashout epoch can occur, with zero juice delivery, resetting the interval
524 before juice can be delivered again. **(C)** State value versus task epoch for a single cue condition
525 +2 vs +1. As the model proceeds through a trial, state value changes depending on task epoch
526 and outcome. In this example, there is one token at fixation (red dot, far left) and three traces
527 are shown, one to represent each possible outcome (+2 tokens, +1 token, 0 token change).
528 State value increases for gaining tokens and decreases slightly when no tokens are gained.
529 State value at cashout corresponds to the token count. The state value is identical for all three
530 outcome traces during the intertrial interval after a cashout. **(D)** State value versus task epoch
531 for a single cue condition -2 vs -1. In this example, there are two tokens at fixation (red dots, far
532 left) and three traces are shown, one to represent each possible outcome (-2 tokens, -1 token, 0
533 token change). State value decreases when tokens are lost and stays constant when the
534 outcome is zero tokens. At the time of cashout, state value depends on whether tokens are
535 present. Like in (C), the state value is identical for all three outcome traces during the intertrial
536 interval after a cashout. **(E)** Cue state value (V_{cue}) versus number of observations of a cue pair
537 (NObs). As NObs increases, the state value increases for all cue conditions that include the
538 best option (+2 tokens). The state value for the cue conditions with the +1 option decreases with
539 learning and plateaus. The state value for the loss vs. loss condition (-2 v -1) decreases with
540 NObs. **(F)** Fixation state value versus NObs. As NObs increases, the value of the fixation state
541 increases. As the monkey proceeds through a block, they learn the associations between the
542 cue images and token outcomes, and it is more likely the monkey will select the better options
543 (+2 and +1). In the MDP, this means that as NObs increases, it will be more likely that tokens
544 will be received, which causes an increase in the future expected value and thus state value.
545

546 knows which cues correspond to +2 and +1 tokens (e.g. NObs 18), the state action
547 values will reflect the knowledge of the best option and the state values at the time of
548 the cue state will be higher for the conditions with +2 or +1 cues (**Fig. 4E**). Even though
549 the fixation state precedes the cue state, the number of observations also affects the
550 value of the fixation state and causes it to increase as NObs increases, because the
551 monkey can make better choices when the options are presented (**Fig. 4F**). The
552 minimum state value is at the baseline for all features, i.e. NTk=0, TSCO=1,
553 TE=Fixation, NObs=1 (**Fig. 4F**, NObs=1).

554 The exact value of the baseline state value and the relationship between NObs
555 and the fixation state value vary by model (i.e. monkey). This relationship is affected by
556 three things: the token outcome transition probabilities, the discount factor, and number
557 of iterations for fitting the model. The discount factor was 0.999 for all monkeys, and the
558 number of iterations for fitting each model was constant. Only the token outcome
559 transition probabilities ($p_{\text{Atk}|\text{choice}}$), which were fit to each monkey's behavior, vary
560 between monkeys in the models. Therefore, the larger the token outcome transition
561 probabilities to gain outcomes, the larger the initial state value even at the time of
562 fixation. In other words, when the monkey learned faster, these transition probabilities
563 changed faster, and state value increased faster with NObs.

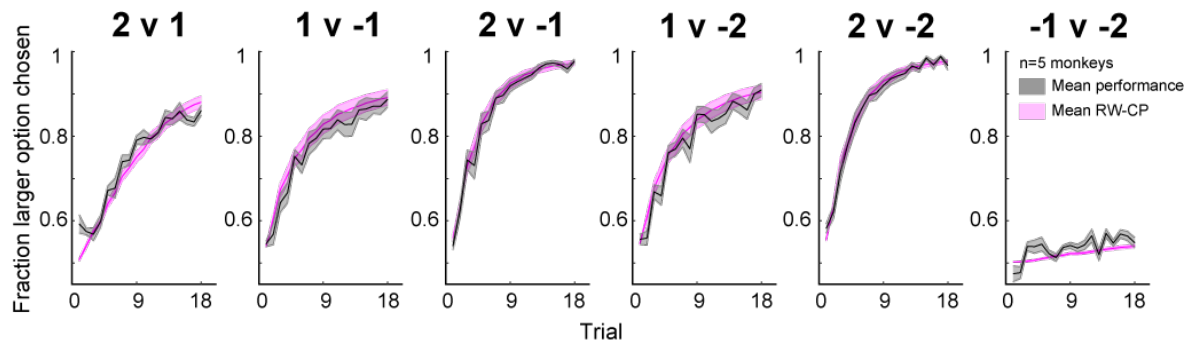
564

565 **State-based MDP model of symbolic reinforcement captures learning behavior**

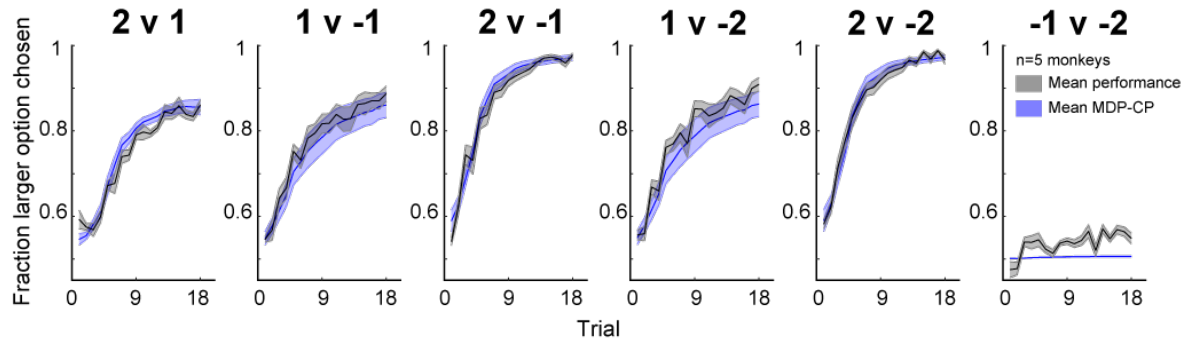
566 To test the validity of the choice policy of the MDP model for each monkey, we
567 calculated the choice probabilities produced by the choice policy of each MDP, after
568 passing action values through a softmax. After fitting an MDP to each monkey, choice
569 probability was calculated using the action values for each choice in each cue condition,
570 for each trial in a block (NObs 1-18). The action values were passed through a softmax
571 with an inverse temperature parameter β (see methods), which controlled the
572 stochasticity of the choice policy given two action values. Average choice probability
573 across animals demonstrated that the choice probabilities produced by the MDP
574 produced similar fits to the behavioral data to the RW-RL model, with no statistically
575 significant difference between the correlation coefficients computed from the behavioral
576 data and the two models ($r_{\text{RW}} = 0.9904$, $r_{\text{MDP}} = 0.9868$, difference in correlation: $p = 0.25$,

577 **Fig. 5).** This verified that the MDP captures choice behavior in the task, over and above
578 its ability to model future state values. Further analyses using state values are,
579 therefore, grounded in an accurate representation of choice behavior.

A



B

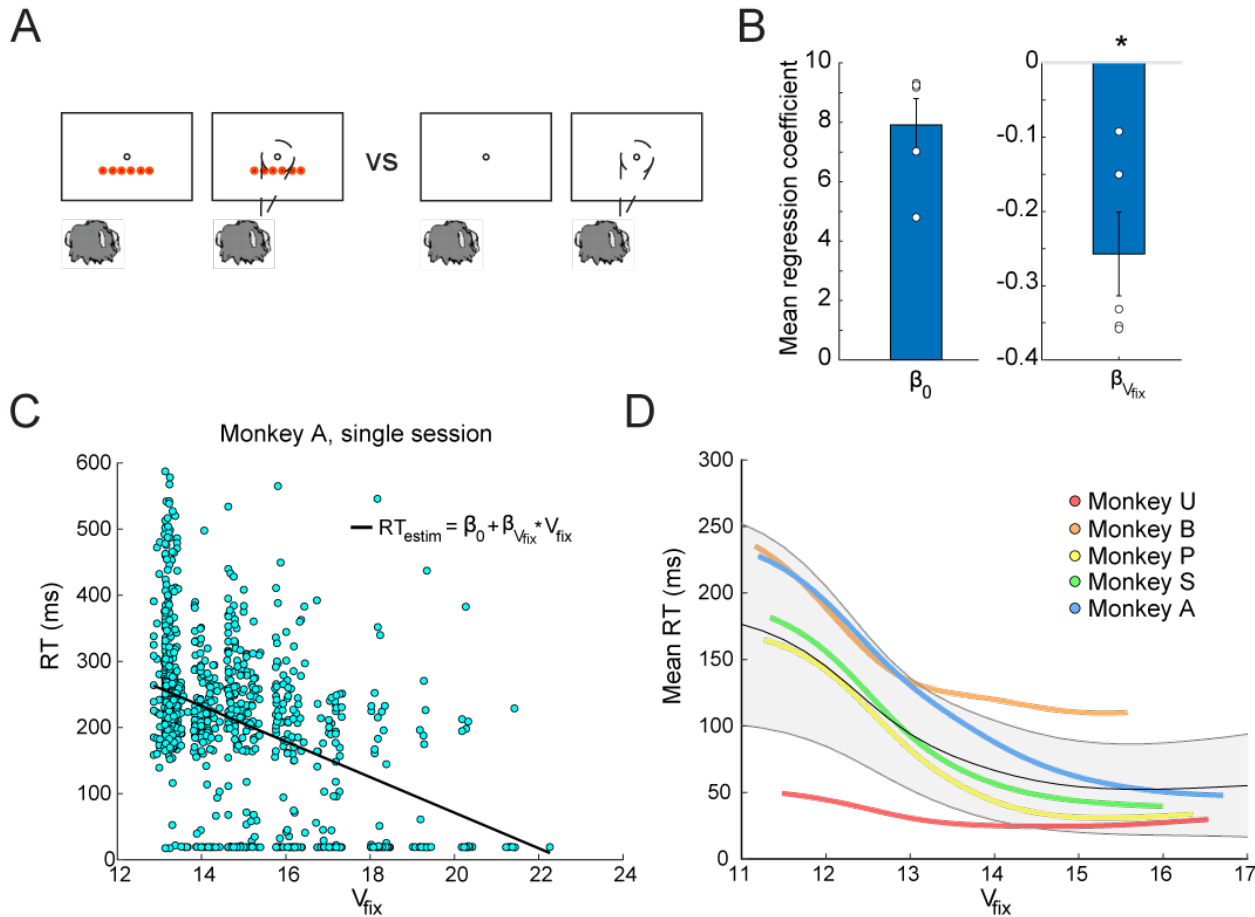


580
581 **Figure 5. Average performance in the tokens task and model fits. (A)** Average performance
582 and RW-RL model fits for all subjects (n=5) monkeys in the six task conditions (s.e.m. across
583 animals). **(B)** Same as (A) but average MDP choice probability instead of RW-RL model fits.
584

585 **Time to acquire fixation is related to the value of the fixation state**

586 We next examined whether the MDP state values could be used to predict
587 motivation in monkey behavior. The first question was how state value might affect the
588 initiation of a trial, which has been previously shown to be affected by motivation (Hamid
589 et al., 2016; Oemisch, Johnston and Paré, 2016; Mohebi et al., 2019; Steinmetz et al.,
590 2019). For example, if the monkey has multiple tokens at the start of a trial, might they
591 be more motivated to initiate a trial, than in the case when they have no tokens (**Fig.**

592 **6A)**? However, token count is not the only task feature that could affect motivation in
593 this task. Thus, we used the value of the fixation state (V_{fix}) from the MDP to relate all
594 relevant task features (NTk, TSCO, TE, NObs) on a trial-by-trial basis to the time it took



596 **Figure 6. Reaction time to acquire fixation.** **(A)** An example case of when motivation might
597 differ in the tokens task at the time of fixation. **(B)** Mean regression coefficients across animals
598 from the linear regression on V_{fix} (bar plot) and mean beta values across sessions for each
599 animal (dots). (* indicates $p < 0.05$). Note that regressions were conducted on $\log(RT)$. **(C)** An
600 example set of reaction times from a single session from Monkey A showing a decrease in
601 reaction time to acquire fixation as V_{fix} increases with an overlay of the regression line. Values
602 near zero indicate trials in which the monkey was already within the fixation window when the
603 fixation cue appeared. **(D)** Kernel smoothed, averaged mean reaction times for each monkey
604 versus V_{fix} . Average reaction times across sessions are shown for each animal in a different
605 color indicated by the legend. The average of all animals is shown in grey, with error bars
606 showing the standard deviation across animals.

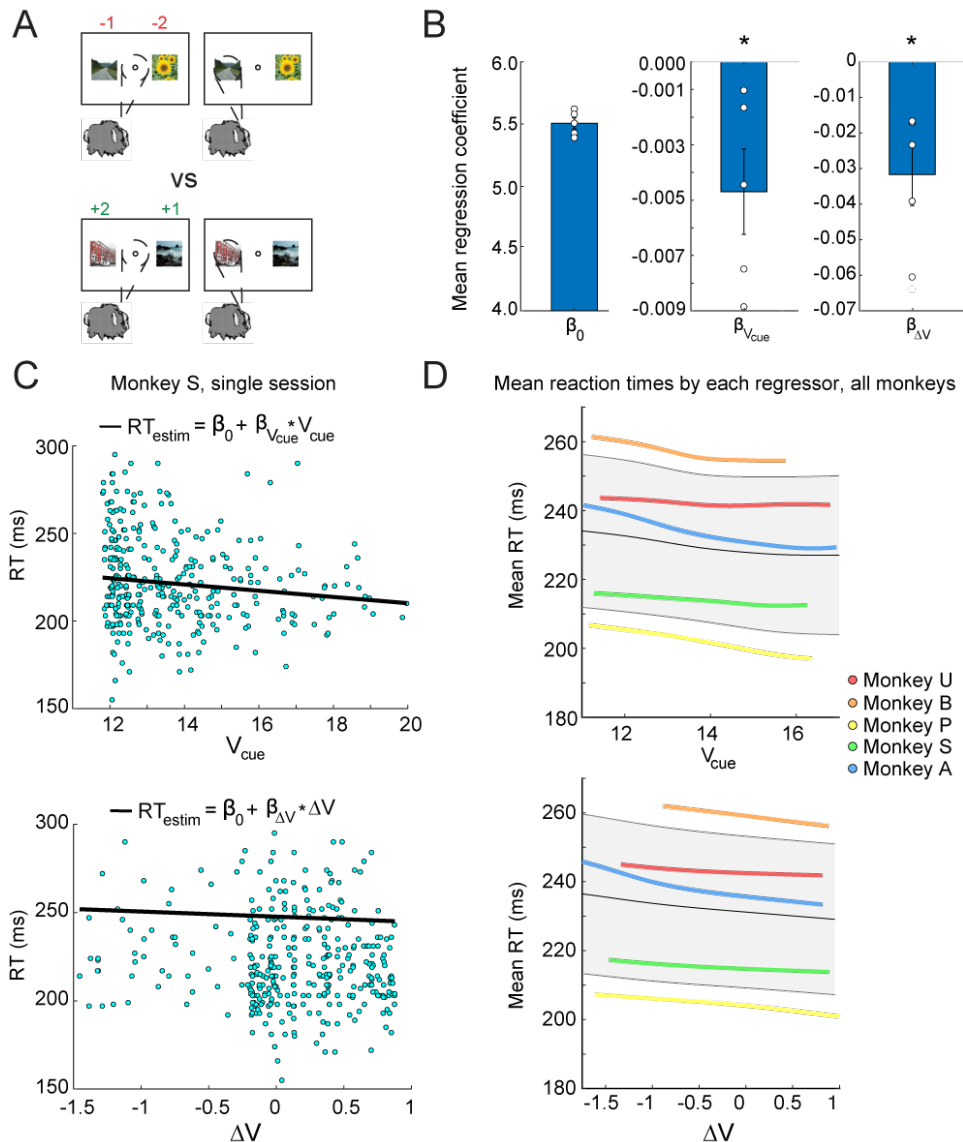
607
608 the animal to acquire the fixation spot. We conducted a linear regression for each
609 session of data from each animal and calculated the average regression coefficient

610 value for each animal (**Fig. 6B**). Mean regression coefficients for V_{fix} ($\beta_{V_{fix}}$) were
611 significantly less than zero at the group level ($p= 0.0312$, Wilcoxon signed-rank test). All
612 five of the individual distributions of regression coefficients for each animal were
613 statistically significant ($t(20)= -5.78$; $t(22)= -9.48$; $t(16)= -11.74$; $t(19)= -28.18$; $t(19)= -$
614 19.37 ; $p<0.0001$). Thus, as the value of the fixation state increased, reaction times
615 decreased (**Fig. 6C**) and this was true for all five monkeys (**Fig. 6B, 6D**).

616

617 **Choice reaction time is related to the value of the cue state and change in state**
618 **value**

619 Next, we asked whether choice reaction times were related to the value of the
620 cue state (V_{cue}) and the change in value between the cue onset and fixation state ($\Delta V=$
621 $V_{cue} - V_{fix}$), which would reflect an impending gain or loss of tokens from selecting a cue.
622 For example, if the cue condition was loss v. loss (-1 vs. -2), the monkey might be
623 slower to choose an option than in the case of gain v. gain (+1 vs. +2) where there is a
624 preferred option (**Fig. 7A**). We conducted a linear regression of V_{cue} and ΔV on reaction
625 times for each session of data from each animal and calculated the average regression
626 coefficient for each animal (**Fig. 7B**). Mean regression coefficients $\beta_{V_{cue}}$ and $\beta_{\Delta V}$ were
627 significantly less than zero at the group level ($p= 0.0312$, Wilcoxon signed-rank test).
628 This meant that as the value of the cue state increased, reaction times became faster,
629 and as the change in cue value became more positive, reaction times also



630

631 **Figure 7. Reaction time to choice. (A)** An example case of when motivation might differ in the
 632 tokens task at the time of image cue presentation. Image credit: Wikimedia Commons (scene
 633 images). **(B)** Mean regression coefficients cross animals from the linear regression on V_{cue} and
 634 ΔV (bar plots) and mean beta values across sessions for each animal (dots). (*) indicates $p <$
 635 0.05). Note that regressions were conducted on $\log(RT)$. **(C)** Example set of reaction times from
 636 a single session from Monkey S showing a decrease in choice reaction time as V_{cue} increases
 637 and ΔV becomes more positive with regression fits overlaid. **(D)** Kernel smoothed, averaged
 638 mean reaction times for each monkey versus V_{cue} and ΔV . Average reaction times across
 639 sessions are shown for each animal in a different color indicated by the legend. The average of
 640 all animals is shown in grey, with error bars showing the standard deviation across animals.
 641

642 became faster (Fig 7C, 7D). Four of the five individual monkey distributions of β_{Vcue} ,
 643 where session was the repeat, were statistically significant ($t(20) = -2.19$, $p < 0.05$; $t(22) =$

644 -6.62, $p <0.0001$; $t(16) = -3.44$, $p <0.005$; $t(19) = -1.98$, $p =0.06$; $t(19) = -14.78$, p
645 <0.0001). Five of the five individual distributions of $\beta_{\Delta V}$ were statistically significant
646 $t(20) = -7.29$, $p <0.0001$; $t(22) = -8.86$, $p <0.0001$; $t(16) = -3.22$, $p <0.01$; $t(19) = -3.89$, p
647 <0.001 ; $t(19) = -9.98$, $p <0.0001$). In summary, this demonstrated that as the value of
648 the cue state was higher, choice reaction times were faster for all animals. These
649 analyses also demonstrated that when the change in state value from fixation to cue
650 (ΔV) was positive, reaction times were also faster.

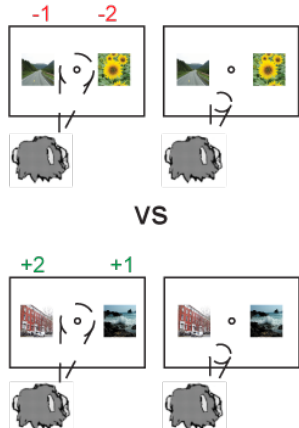
651

652 **The probability of the monkey aborting a trial is related to the value of the cue**
653 **state**

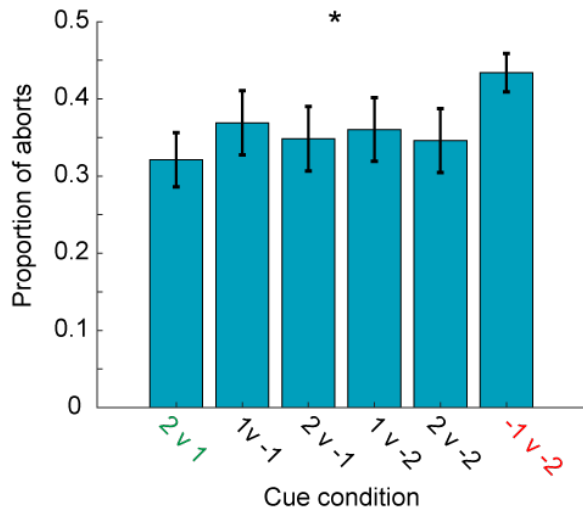
654 To investigate the relationship between the completion of a trial and state value,
655 we related the frequency of trial aborts to state value by looking at all trials in a session
656 and analyzing both complete and incomplete trials. If the monkey moved his eyes
657 outside the fixation window during fixation, did not choose a cue, or did not hold the cue
658 long enough, the trial was aborted and repeated. Given that the monkeys do not learn to
659 pick the smaller loss well in the loss vs. loss condition (Fig. 5), it might be more likely
660 that the animal aborts these trials to avoid losing tokens (Fig. 8A). Indeed, past work
661 has shown that monkeys are more likely to abort cue conditions with two loss cues
662 (Taswell et al., 2018). We found a significant effect of cue condition on the frequency of
663 aborts (mixed effects ANOVA, main effect: cue condition $F(5, 29) = 7.86$, $p <0.001$;
664 random effect: monkey $F(4, 29) = 51.14$) (Fig. 8B). We next asked whether cue state
665 value and changes in state value were related to the probability of aborting a trial by

666 conducting logistical regression on cue state value (V_{cue}) and the change in value
 667 between the cue state and

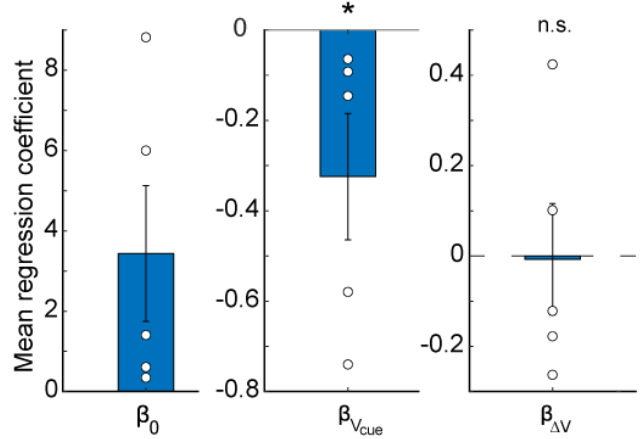
A



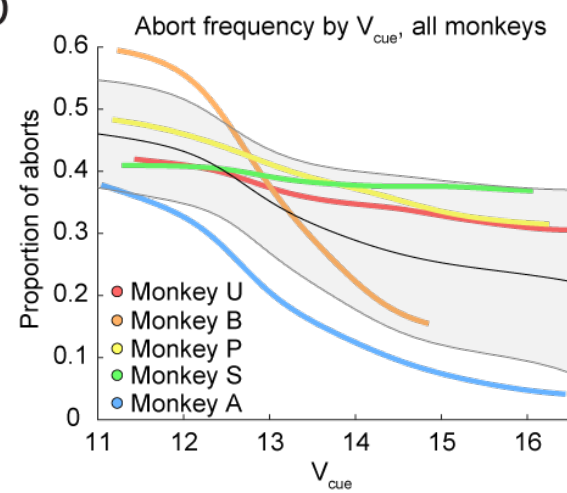
B



C



D



668

669 **Figure 8. Probability of aborting a trial.** (A) An example case of when motivation to complete
 670 a trial might differ in the tokens task at the time of image cue presentation. Image credit:
 671 Wikimedia Commons (scene images). (B) Average proportion of aborts in each task condition
 672 (s.e.m. average across n=5 monkeys, * indicates p< 0.05). (C) Mean regression coefficients
 673 across animals for the logistic regression on V_{cue} and ΔV . Only the regressor for V_{cue} was
 674 statistically significant. (D) Kernel smoothed, averaged mean reaction times for each monkey
 675 versus V_{cue} . Average proportions of aborts across sessions are shown for each animal in a
 676 different color indicated by the legend. The average of all animals is shown in grey, with error
 677 bars showing the standard deviation across animals.
 678

679 fixation state ($\Delta V = V_{cue} - V_{fix}$). The distribution of mean regression coefficients $\beta_{V_{cue}}$ was
680 significantly less than zero at the group level ($p = 0.0312$, Wilcoxon signed-rank test)
681 whereas $\beta_{\Delta V}$ did not emerge as significant ($p = 0.4062$, Wilcoxon signed-rank test),
682 suggesting that changes in state value were not the main factor related to abort
683 behavior (**Fig. 8C**). Four of the five individual distributions of $\beta_{V_{cue}}$ were statistically
684 significant ($t(20) = -3.33$, $p < 0.01$; $t(22) = -19.78$, $p < 0.0001$; $t(16) = -3.46$, $p < 0.01$; $t(19) = -$
685 1.94 , $p = 0.068$; $t(19) = -14.78$, $p < 0.0001$). Overall trends across animals showed that
686 as the value of the cue state increased, the probability of aborting decreased (**Fig. 8D**).
687

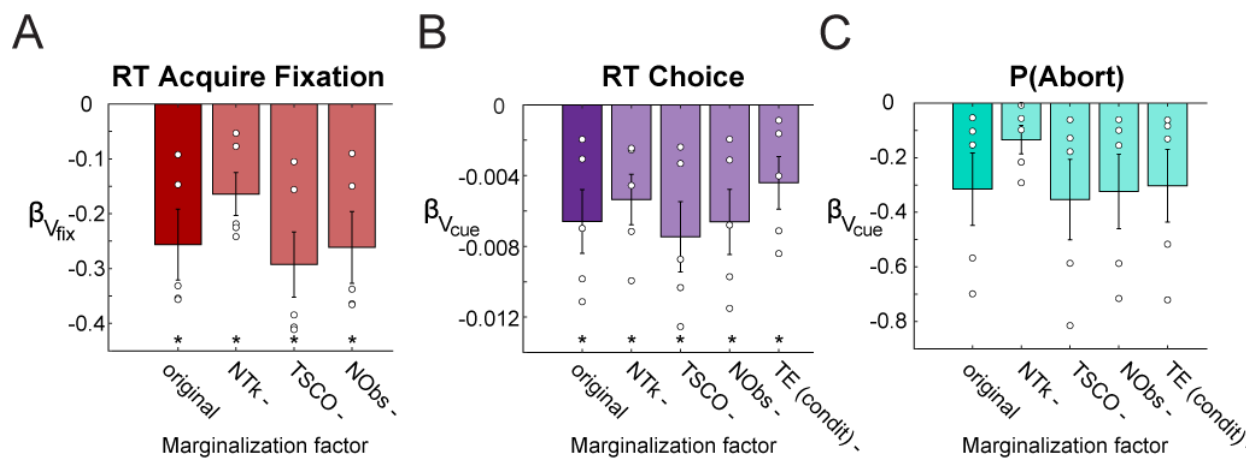
688 **All MDP state features contribute to state values**

689 We next examined whether token count was the only driving force for the
690 correlations found between state values and behavior. As was shown, current token
691 count strongly influenced state value (Fig. 4). To assess the contribution of each of the
692 features in the MDP to the regression results, we marginalized across each feature,
693 thus removing the effect of variation in that feature on state value, and recomputed the
694 regressions. For example, to marginalize over token count, state values for each trial
695 were extracted using only the other features (TSCO, TE, NObs) after averaging over the
696 values for all possible values of token count. The average of these state values was
697 used as the single trial state value for the regressions.

698 For reaction time to acquire fixation, all distributions of regression coefficients
699 remained statistically significant for each marginalized version of the regression (**Fig.**
700 **9A**). Removing token count from the regression had the largest effect on reducing the
701 relationship between V_{fix} and reaction time to acquire fixation. Removing TSCO and

702 NObs in the regression for reaction time to acquire led to an increase in beta values,
703 which suggests these factors interact and affect the regression, but are less important
704 than token count in the regression. For both choice reaction time and probability of
705 aborting a trial, regressions were recomputed using only one regressor, for V_{cue} . This
706 was because removing the cue condition from the regression caused $\Delta V = V_{cue} - V_{fix}$ to go
707 to zero and therefore made the regressions uninterpretable. Marginalizing over cue
708 condition or tokens in the regression for choice reaction times reduced the magnitude of
709 the regression coefficients (Fig. 9B). This reflects a weaker relationship between the
710 state value and reaction times without these features. In the logistic regression for
711 aborts, marginalizing over tokens also had the largest effect on the regressors, but did
712 not eliminate the relationship between state value and the probability of aborting a trial
713 (Fig. 9C). Taken together, these analyses show that the number of tokens strongly
714 affects all behavioral measures but is not the only factor leading to the relationships
715 between behavior and state value.

716



717
718 **Figure 9. Marginalization over features.** Linear regressions for each behavioral feature were
719 recomputed using state values that omitted the effect of a single feature at a time: number of
720 tokens (NTk), trials since cashout (TSCO), number of observations of a cue pair (NObs), Task

721 Epoch (TE, condit). Mean regression coefficients across animals are shown (bar plots) and for
722 each subject (dots) for three behavioral features: **(A)** RT to acquire fixation **(B)** RT to choice **(C)**
723 Probability of aborting trials. Error bars s.e.m.

724

725 **Discussion**

726 In this study, monkeys learned to make choices to maximize gains and minimize
727 losses of tokens. The tokens were symbolic reinforcers that represented future juice
728 rewards. We designed a Markov Decision Process (MDP) model to capture the
729 relationship between features of the task that drive behavior (i.e. states) and value. We
730 then related these state values to measures of motivation. The state space for the task
731 included the number of tokens (NTk), trials since cashout (TSCO), task epoch (TE), and
732 the number of observations of each cue pair (NObs). We found that reaction times to
733 acquire fixation, choice reaction times, and the probability of aborting a trial were
734 significantly related to state value and changes in state value (except abort probability).
735 Furthermore, we demonstrated that state values were dependent on all state features,
736 not just the number of tokens. Number of tokens did, however, often have a large
737 effect. These relationships between state value and behavior cannot be captured by
738 simpler models such as the Rescorla-Wagner model, as these models are stateless and
739 therefore cannot capture state values that depend on future rewards, nor can they
740 account separately for tokens vs. primary rewards. Given that the MDP also allows for
741 modeling trial state-dependent values, it can also be used in future work to understand
742 the neural circuitry relevant to the task.

743 Past work has shown that symbolic (or secondary) reinforcers can drive learning
744 and have motivational properties similar to those of primary rewards (Wolfe, 1936;
745 Wyckoff, 1959; Jackson, 1996; Sousa and Matsuzawa, 2001; Seo and Lee, 2009;

746 Donahue and Lee, 2015; Farashahi et al., 2018; Taswell et al., 2018; Beran and
747 Parrish, 2021; Yang, Li and Stuphorn, 2022; Taswell et al., 2023). This happens through
748 the learned associations between tokens and primary reinforcers. In this task, tokens
749 and cue images both predict rewards, although in different ways. Cues are
750 stochastically linked to tokens on short timescales, whereas tokens are deterministically
751 linked to juice on longer timescales. Cues, therefore, predict rewards, but only through
752 tokens. The cues also change in each block, which requires rapid learning of the cue
753 values, whereas the relationship between tokens and juice is stable and constant over
754 the course of the experiment. The state-based modeling framework presented here
755 accounts for the differential attributes of cues and tokens and allows for examining
756 behavioral measures related to motivation, including trial initiation time, choice reaction
757 times, and trial aborts.

758 The time to initiate a trial has been studied previously as a measure of motivation
759 (Hamid et al., 2016; Oemisch, Johnston and Paré, 2016; Mohebi et al., 2019; Steinmetz
760 et al., 2019). In a task which required rodents to nose poke after a light went on, rodents
761 were faster, interpreted as increased motivation, when reward rate was higher (Hamid
762 et al., 2016; Mohebi et al., 2019). When we investigated the relationship between state
763 value and reaction times to acquire fixation, we found that a higher state value
764 correlated with faster reaction times to acquire fixation. This implies a somewhat
765 counterintuitive result: that on the trials immediately after receiving reward (during
766 cashout), when state value is lowest, the monkeys are, on average, slower to initiate the
767 next trial. Thus, symbolic reinforcers have assumed the motivational properties of
768 rewards to encourage the choice to begin work.

769 Past work on choice reaction times has also suggested that reward expectation
770 can influence execution of a choice response (Hollerman, Tremblay and Schultz, 1998;
771 Wräse et al., 2007). Our regressions on cue state value and changes in state value from
772 fixation suggested that reaction times to choose options were affected by other task
773 factors, including distance to cashout, the number of tokens present, and the desirability
774 or value of the cue condition. This fits with past work that has shown that expected
775 outcomes can affect reaction times (Hollerman, Tremblay and Schultz, 1998; Shidara,
776 Aigner and Richmond, 1998). In the Tokens task, once the monkeys knew the values of
777 the cue images, the images served as a similar instruction to the possible outcomes as
778 in past studies. Regressions on cue state value showed that as cue state value
779 increased, reaction times decreased, as the monkeys learned to anticipate gains from
780 certain cue conditions. Correspondingly, in loss vs. loss (-2 v -1) trials, the monkeys
781 slowed their choices.

782 Aborted trials can happen for many reasons. In our Tokens task, however, we
783 observed a systematic increase in abort trials in the condition involving only loss options
784 (-2 v -1), which led us to investigate how cue state value and changes in state value
785 might correlate with this behavior. Past work on trial abort behavior has shown that
786 aborts (or refusals) occur most often in trials furthest from reward (La Camera and
787 Richmond, 2008; Inaba et al., 2013) and trials that require the most effort (Pasquereau
788 and Turner, 2013, 2015; Varazzani et al., 2015), suggesting that animals are more
789 motivated to complete a trial when the cost of reaching a reward is lower. Our
790 regression results are consistent with these findings, as monkeys were less likely to
791 abort when the cue state value was higher.

792 Our analysis showed that monkeys were motivated to work when they had more
793 tokens. However, as our marginalization over dimensions of the state vector showed,
794 state values and our regression results depend on more than the number of tokens
795 present. In this task, higher state value, and therefore higher discounted future expected
796 reward, led to faster trial initiation, faster reaction times, and fewer aborts. This has
797 implications for understanding the neural responses, as the time leading up to the
798 receipt of the reward, also known as the anticipatory phase (Knutson et al., 2001; Ernst
799 et al., 2004; Rademacher et al., 2017), has signals that capture expectation of future
800 reward, which occurs in the consummatory phase (Dillon et al., 2008; Kumar et al.,
801 2014). Understanding the dynamics of anticipation, motivation, and reward in a single
802 framework allows for linking both processes to fluctuations in neural activity in multiple
803 brain areas.

804 Within the presented framework, symbolic reinforcers have been recast as
805 dimensions that drive state value. Past work involving choice tasks and state value have
806 suggested the existence of a ventral circuit for the representation of state value
807 (Gläscher et al., 2010; Averbeck and Murray, 2020) and state transitions (Belova, Paton
808 and Salzman, 2008; Chan et al., 2021; Kalmbach et al., 2022). It has been
809 hypothesized that distinct ventral and dorsal networks define behavioral goals and
810 orchestrate actions to achieve goals, respectively (Everitt et al., 1999; Cardinal et al.,
811 2002; Averbeck and Costa, 2017; Averbeck and Murray, 2020). In choice tasks, the
812 main behavioral goal is to reach high value states. Recent work has shown correlations
813 between fluctuations in dopamine and state value (Hamid et al., 2016), and local control
814 of dopamine in the ventral striatum, is related to motivation (Mohebi et al., 2019).

815 However, the ventral circuit, which includes the orbital frontal cortex, ventral medial
816 prefrontal cortex, ventral striatum, ventral pallidum, and amygdala, is innervated by
817 dopaminergic projections in multiple sites (Haber, 2014), and thus dopamine may
818 differentially affect processing in each of these areas to support reinforcement learning
819 and motivation (Berke, 2018; Westbrook and Frank, 2018). Furthermore, recent lesion
820 work has shown that lesions of the ventral striatum and amygdala show only subtle
821 deficits on performance on the Tokens task (Taswell et al., 2018; Taswell et al., 2023)
822 but larger deficits in reversal learning tasks (Costa et al., 2016) and tasks requiring
823 switches between action-based and stimulus-based strategies (Rothenhoefer et al.,
824 2017).

825 The question then becomes, how are connections between symbolic
826 reinforcement, rewards, and actions represented in the brain? Symbolic reinforcers
827 such as tokens could be tracked directly across multiple areas, as a global
828 representation of visual object numerosity (Tudusciuc and Nieder, 2009; Ramirez-
829 Cardenas, Moskaleva and Nieder, 2016; Viswanathan and Nieder, 2020), but
830 numerosity does not directly have motivational value. However, symbolic reinforcers
831 can take on a range of identities. Furthermore, other states including abstract
832 completion of intermediate goals can serve as symbolic reinforcers (Janssen et al.,
833 2022). Furthermore, as the capacity to measure more neural signals simultaneously has
834 advanced, there has been growing evidence that task-related signals are represented
835 across many areas (Dotson et al., 2018; Steinmetz et al., 2019; Fine et al., 2023).
836 Therefore, it is unlikely that there would be a localized neural signature of an individual
837 task feature, as most task features will be represented across many areas. Thus, we

838 must consider how symbolic reinforcers might be mapped onto a distributed
839 representation that allows for flexibility in the identity of the reinforcer, and design future
840 experiments with this in mind. Here, we have selected four features to integrate: tokens,
841 temporal distance to reward, task epoch, and cue observations to measure the state
842 value moment by moment in the task. The model therefore generates values for each
843 task state, including fixation, cue presentation, token outcome, and the inter-trial
844 interval.

845 In summary, we developed a computational framework that quantifies the value
846 of symbolic reinforcers and characterizes the effect of several task features on those
847 values. Furthermore, the model captures not only choice behavior, but also behaviors
848 related to motivation. In this task, reaction times to initiate a trial, choice reaction times,
849 and the probability of completing a trial were correlated with state value and changes in
850 state value. Our results suggest that symbolic reinforcers and rewards can have similar
851 effects on behavior, which allows for predictions about how symbolic reinforcers might
852 be represented in the brain.

853

854 **References:**

855 Asaad WF, Eskandar EN (2008) A flexible software tool for temporally-precise behavioral control
856 in Matlab. *Journal of neuroscience methods* 174:245-258.
857 Averbeck BB, Costa VD (2017) Motivational neural circuits underlying reinforcement learning.
858 *Nat Neurosci* 20:505-512.

859 Averbeck BB, Murray EA (2020) Hypothalamic Interactions with Large-Scale Neural Circuits
860 Underlying Reinforcement Learning and Motivated Behavior. *Trends Neurosci* 43:681-
861 694.

862 Bartolo R, Averbeck BB (2020) Prefrontal Cortex Predicts State Switches during Reversal
863 Learning. *Neuron* 106:1044-1054 e1044.

864 Belova MA, Paton JJ, Salzman CD (2008) Moment-to-moment tracking of state value in the
865 amygdala. *Journal of Neuroscience* 28:10023-10030.

866 Beran MJ, Parrish AE (2021) Non-human primate token use shows possibilities but also
867 limitations for establishing a form of currency. *Philos Trans R Soc Lond B Biol Sci*
868 376:20190675.

869 Berke JD (2018) What does dopamine mean? *Nature Neuroscience* 21:787-793.

870 Beron CC, Neufeld SQ, Linderman SW, Sabatini BL (2022) Mice exhibit stochastic and efficient
871 action switching during probabilistic decision making. *Proceedings of the National
872 Academy of Sciences* 119.

873 Berridge KC (2004) Motivation concepts in behavioral neuroscience. *Physiology & Behavior*
874 81:179-209.

875 Cardinal RN, Parkinson JA, Hall J, Everitt BJ (2002) Emotion and motivation: the role of the
876 amygdala, ventral striatum, and prefrontal cortex. *Neuroscience & Biobehavioral
877 Reviews* 26:321-352.

878 Chan SCY, Schuck NW, Lopatina N, Schoenbaum G, Niv Y (2021) Orbitofrontal cortex and
879 learning predictions of state transitions. *Behav Neurosci* 135:487-497.

880 Costa VD, Dal Monte O, Lucas DR, Murray EA, Averbeck BB (2016) Amygdala and Ventral
881 Striatum Make Distinct Contributions to Reinforcement Learning. *Neuron* 92:505-517.

882 Delgado M, Jou R, Phelps E (2011) Neural Systems Underlying Aversive Conditioning in Humans
883 with Primary and Secondary Reinforcers. *Frontiers in Neuroscience* 5.

884 Dillon DG, Holmes AJ, Jahn AL, Bogdan R, Wald LL, Pizzagalli DA (2008) Dissociation of neural
885 regions associated with anticipatory versus consummatory phases of incentive
886 processing. *Psychophysiology* 45:36-49.

887 Donahue CH, Lee D (2015) Dynamic routing of task-relevant signals for decision making in
888 dorsolateral prefrontal cortex. *Nature Neuroscience* 18:295-301.

889 Dotson NM, Hoffman SJ, Goodell B, Gray CM (2018) Feature-based visual short-term memory is
890 widely distributed and hierarchically organized. *Neuron* 99:215-226. e214.

891 Ernst M, Nelson EE, McClure EB, Monk CS, Munson S, Eshel N, Zarahn E, Leibenluft E, Zametkin
892 A, Towbin K, Blair J, Charney D, Pine DS (2004) Choice selection and reward anticipation:
893 an fMRI study. *Neuropsychologia* 42:1585-1597.

894 Everitt BJ, Parkinson JA, Olmstead MC, Arroyo M, Robledo P, Robbins TW (1999) Associative
895 Processes in Addiction and Reward The Role of Amygdala-Ventral Striatal Subsystems.
896 *Annals of the New York Academy of Sciences* 877:412-438.

897 Falligant JM, Kranak MP (2022) Rate Dependence and Token Reinforcement? A Preliminary
898 Analysis. *The Psychological Record* 72:751-757.

899 Farashahi S, Azab H, Hayden B, Soltani A (2018) On the Flexibility of Basic Risk Attitudes in
900 Monkeys. *J Neurosci* 38:4383-4398.

901 Fine JM, Maisson DJ-N, Yoo SBM, Cash-Padgett TV, Wang MZ, Zimmermann J, Hayden BY (2023)

902 Abstract Value Encoding in Neural Populations But Not Single Neurons. *The Journal of*
903 *Neuroscience* 43:4650-4663.

904 Gläscher J, Daw N, Dayan P, O'Doherty JP (2010) States versus rewards: dissociable neural
905 prediction error signals underlying model-based and model-free reinforcement learning.

906 *Neuron* 66:585-595.

907 Haber SN (2014) The place of dopamine in the cortico-basal ganglia circuit. *Neuroscience*
908 282:248-257.

909 Hackenberg TD (2009) Token reinforcement: A review and analysis. *Journal of the experimental*
910 *analysis of behavior* 91:257-286.

911 Hackenberg TD (2018) Token reinforcement: Translational research and application. *Journal of*
912 *applied behavior analysis* 51:393-435.

913 Hamid AA, Pettibone JR, Mabrouk OS, Hetrick VL, Schmidt R, Vander Weele CM, Kennedy RT,
914 Aragona BJ, Berke JD (2016) Mesolimbic dopamine signals the value of work. *Nat*
915 *Neurosci* 19:117-126.

916 Hayden BY, Niv Y (2021) The case against economic values in the orbitofrontal cortex (or
917 anywhere else in the brain). *Behavioral Neuroscience* 135:192-201.

918 Hollerman JR, Tremblay L, Schultz W (1998) Influence of Reward Expectation on Behavior-
919 Related Neuronal Activity in Primate Striatum. *Journal of Neurophysiology* 80:947-963.

920 Hwang J, Mitz AR, Murray EA (2019) NIMH MonkeyLogic: Behavioral control and data
921 acquisition in MATLAB. *Journal of neuroscience methods* 323:13-21.

922 Inaba K, Mizuhiki T, Setogawa T, Toda K, Richmond BJ, Shidara M (2013) Neurons in Monkey
923 Dorsal Raphe Nucleus Code Beginning and Progress of Step-by-Step Schedule, Reward
924 Expectation, and Amount of Reward Outcome in the Reward Schedule Task. *The Journal*
925 of Neuroscience 33:3477-3491.

926 Jackson KH, T (1996) Token Reinforcement, Choice and Self-control in pigeons.

927 Janssen M, LeWarne C, Burk D, Averbeck BB (2022) Hierarchical Reinforcement Learning,
928 Sequential Behavior, and the Dorsal Frontostriatal System. *Journal of Cognitive*
929 *Neuroscience* 34:1307-1325.

930 Kalmbach A, Winiger V, Jeong N, Asok A, Gallistel CR, Balsam PD, Simpson EH (2022) Dopamine
931 encodes real-time reward availability and transitions between reward availability states
932 on different timescales. *Nature Communications* 13:3805.

933 Kirsch P, Schienle A, Stark R, Sammer G, Blecker C, Walter B, Ott U, Burkart J, Vaitl D (2003)
934 Anticipation of reward in a nonaversive differential conditioning paradigm and the brain
935 reward system:: an event-related fMRI study. *NeuroImage* 20:1086-1095.

936 Knutson B, Adams CM, Fong GW, Hommer D (2001) Anticipation of increasing monetary reward
937 selectively recruits nucleus accumbens. *J Neurosci* 21:Rc159.

938 Kumar P, Berghorst LH, Nickerson LD, Dutra SJ, Goer F, Greve D, Pizzagalli DA (2014) Differential
939 effects of acute stress on anticipatory and consummatory phases of reward processing.
940 *Neuroscience* 266:1-12.

941 La Camera G, Richmond BJ (2008) Modeling the violation of reward maximization and
942 invariance in reinforcement schedules. *PLoS computational biology* 4:e1000131.

943 Mohebi A, Pettibone JR, Hamid AA, Wong J-MT, Vinson LT, Patriarchi T, Tian L, Kennedy RT,

944 Berke JD (2019) Dissociable dopamine dynamics for learning and motivation. *Nature*

945 570:65-70.

946 O'Reilly RC (2020) Unraveling the mysteries of motivation. *Trends in cognitive sciences* 24:425-

947 434.

948 Oemisch M, Johnston K, Paré M (2016) Methylphenidate does not enhance visual working

949 memory but benefits motivation in macaque monkeys. *Neuropharmacology* 109:223-

950 235.

951 Pasquereau B, Turner RS (2013) Limited Encoding of Effort by Dopamine Neurons in a Cost–

952 Benefit Trade-off Task. *The Journal of Neuroscience* 33:8288-8300.

953 Pasquereau B, Turner RS (2015) Dopamine neurons encode errors in predicting movement

954 trigger occurrence. *Journal of Neurophysiology* 113:1110-1123.

955 Puterman ML (2014) Markov decision processes: discrete stochastic dynamic programming:

956 John Wiley & Sons.

957 Rademacher L, Schulte-Rüther M, Hanewald B, Lammertz S (2017) Reward: From Basic

958 Reinforcers to Anticipation of Social Cues. In: *Social Behavior from Rodents to Humans:*

959 *Neural Foundations and Clinical Implications* (Wöhr M, Krach S, eds), pp 207-221. Cham:

960 Springer International Publishing.

961 Ramirez-Cardenas A, Moskaleva M, Nieder A (2016) Neuronal representation of numerosity

962 zero in the primate parieto-frontal number network. *Current Biology* 26:1285-1294.

963 Recorla RA, & Wagner, A. R. (1972) A Theory of Pavlovian Conditioning: Variations in the

964 Effectiveness of Reinforcement and Nonreinforcement. In: *Classical Conditioning II:*

965 Current Research and Theory (A. H. Black WFP, ed), pp 64-69. New York: Appleton-
966 Century-Crofts.
967 Rothenhoefer KM, Costa VD, Bartolo R, Vicario-Feliciano R, Murray EA, Averbeck BB (2017)
968 Effects of Ventral Striatum Lesions on Stimulus-Based versus Action-Based
969 Reinforcement Learning. *J Neurosci* 37:6902-6914.
970 Seo H, Lee D (2009) Behavioral and neural changes after gains and losses of conditioned
971 reinforcers. *J Neurosci* 29:3627-3641.
972 Shidara M, Aigner TG, Richmond BJ (1998) Neuronal Signals in the Monkey Ventral Striatum
973 Related to Progress through a Predictable Series of Trials. *The Journal of Neuroscience*
974 18:2613-2625.
975 Sousa C, Matsuzawa T (2001) The use of tokens as rewards and tools by chimpanzees (*Pan*
976 *troglodytes*). *Anim Cogn* 4:213-221.
977 Steinmetz NA, Zatka-Haas P, Carandini M, Harris KD (2019) Distributed coding of choice, action
978 and engagement across the mouse brain. *Nature* 576:266-273.
979 Sutton RS, Barto AG (1998) Introduction to reinforcement learning: MIT press Cambridge.
980 Taswell CA, Costa VD, Murray EA, Averbeck BB (2018) Ventral striatum's role in learning from
981 gains and losses. *Proc Natl Acad Sci U S A* 115:E12398-E12406.
982 Taswell CA, Janssen M, Murray EA, Averbeck BB (2023) The motivational role of the ventral
983 striatum and amygdala in learning from gains and losses. *Behavioral Neuroscience*
984 137:268-280.

985 Taswell CA, Costa VD, Basile BM, Pujara MS, Jones B, Manem N, Murray EA, Averbeck BB (2021)

986 Effects of Amygdala Lesions on Object-Based Versus Action-Based Learning in

987 Macaques. *Cereb Cortex* 31:529-546.

988 Tudusciuc O, Nieder A (2009) Contributions of primate prefrontal and posterior parietal cortices

989 to length and numerosity representation. *Journal of neurophysiology* 101:2984-2994.

990 Varazzani C, San-Galli A, Gilardeau S, Bouret S (2015) Noradrenaline and Dopamine Neurons in

991 the Reward/Effort Trade-Off: A Direct Electrophysiological Comparison in Behaving

992 Monkeys. *The Journal of Neuroscience* 35:7866-7877.

993 Viswanathan P, Nieder A (2020) Spatial neuronal integration supports a global representation of

994 visual numerosity in primate association cortices. *Journal of Cognitive Neuroscience*

995 32:1184-1197.

996 Westbrook A, Frank M (2018) Dopamine and proximity in motivation and cognitive control.

997 Current Opinion in Behavioral Sciences 22:28-34.

998 Willenbockel V, Sadr J, Fiset D, Horne GO, Gosselin F, Tanaka JW (2010) Controlling low-level

999 image properties: the SHINE toolbox. *Behavior research methods* 42:671-684.

1000 Wolfe JB (1936) Effectiveness of token rewards for chimpanzees. *Comparative Psychology*

1001 Monographs.

1002 Wrase J, Kahnt T, Schlagenhauf F, Beck A, Cohen MX, Knutson B, Heinz A (2007) Different neural

1003 systems adjust motor behavior in response to reward and punishment. *NeuroImage*

1004 36:1253-1262.

1005 Wyckoff L (1959) Toward a quantitative theory of secondary reinforcement. *Psychological*

1006 *review* 66:68.

1007 Yang Y-P, Li X, Stuphorn V (2022) Primate anterior insular cortex represents economic decision

1008 variables proposed by prospect theory. *Nature Communications* 13.

1009